J. Appl. Comput. Mech., 7(2) (2021) 902-912
DOI: 10.22055/JACM.2021.35332.2630

ISSN: 2383-4536
jacm.scu.ac.ir

Shahid Chamran University of Ahvaz

Journal of Applied and Computational Mechanics

Research Paper

Diffusion-thermo Effects in Stagnation Point Flow of Second Grade Fluid past a Stretching Plate

Sudheer Khan[1], Syed Muhammad Imran[2], Shu Wang[3]

[1] College of Applied Science, Beijing University of Technology, Beijing 100124, P.R. China, Email: soudkayani@hotmail.com

[2] Govt Postgraduate College Attock, Pakistan, Email: syedsiim@gmail.com

[3] College of Applied Science, Beijing University of Technology, Beijing 100124, P.R. China, Email: wangshu@bjut.edu.cn

Received October 07 2020; Revised January 06 2021; Accepted for publication January 06 2021.
Corresponding author: S. Khan (soudkayani@hotmail.com)

Abstract. Transmission of heat and mass in boundary layer flows over stretching surfaces play a significant role in metallurgy and polymer industry. In Current article the assisting and opposing flow of a second grade fluid towards a stretching sheet is analyzed to examine the heat and mass transfer in stagnation point boundary layer flow. Different flow parameters such as concentration, surface temperature and stretching velocity are supposed to variate linearly. The basic transport equations are transformed into non-linear ordinary differential equations by means of boundary layer approximation and similarity transmutations, which are then solved by employing nonlinear shooting (NLS) and Keller-box methods (KBM). These techniques are very useful for solving boundary-layer problems and are applicable to other general situations than that presented current study. The outcomes of velocity, temperature, concentration profile, skin-friction coefficient, heat and mass transfer coefficients are analyzed briefly in graphical and tabular formats. The mass transmission rate was found to be in direct relation with Schmidt number. Moreover, we predict that a rise in Prandtl number leads to a decline in temperature and thermal layer of boundary thickness for both supporting and contrasting flows. The outcomes of this article are important for the analysts in the field of second grade fluids. We believe that the article is very well prepared and the results are original and useful from both theoretical and application point of views.

Keywords: Boundary layer; Stretching sheet; Heat Transfer; Mass transfer; Second-grade fluid.

1. Introduction

The phenomenon of heat and mass transfer due to flowing fluid over a stretched sheet gained lot of popularity amongst thematic approach of researchers in current era. The reason of this popularity is its importance in essential sciences, engineering fields and petroleum industry. Physical aspects of this desire for knowledge can be examined in stretching and contracting of springs, rubber bands, catapults, etc. End products in the extrusion of polymers in shape of polymer sheets and filaments is its example on industrial level. These processes in engineering terminology can be named as stretching sheets and this stretching sheet phenomenon is the foundation milestone in the production of paper, polymer engineering, metal spinning and crystal growing. Heat transfer rate and coefficient of skin friction has greater importance in above mentioned applications because the quality of end product mainly depends on these parameters. Sakiadis [1] was the first who proposed a flow model for stretching mobile surfaces and later Crane [2] presented an analytical solution of a similar model for a viscous fluid. To understand the fluid conduct and experimental approach, a great amount of work has done in the literature to design these problems [3-9]. The familiar Navier- Stokes equations are not suitable to portray the trends in flow of non-Newtonian fluids. So far, several governing systems are recommended in literature because of their protean nature. To examine the effects of normal stress, second grade fluid model kept under consideration. State of the art can be found on these fluids in studies [10–14].

The remarkable implication of the flow near stagnation point and flow over stretchable surfaces have noticed in fluid engineering such as submersible-machinery, hydraulic engines and oil ships, etc. Just beside the stagnation point, the steady patterns of fluid flow were the pioneer work reported by Hiemenz [15]. Chiam [16] investigated that the effect of outspreading near the stagnation withdraws the proclivity to create the boundary layer. Working with micro-polar fluid on the way to a elongating sheet, the normal stagnation stream of fluid was studied by Nazar et al. [17]. Layek et al. [18] scrutinized the passage of mass and heat in the direction of a stretching plate with absorption/emission of heat over boundary layer stagnation-point flow. Nadeem et al. [19] employed the homotopy analysis method (HAM) to attain the outcomes for BLF close to stagnation-place of a stretchable plate. Singh et al. [20] obtained characteristics of nonlinear MHD laminar boundary layer flow by resolving nonlinear ordinary differential equations with HAM technique. Hayat et al. [21] reveal an assumption about linear changes in the thermal state of sheet surface and velocity by examining the mixed convection BLF. Ishak et al. [22] studied mixed convection fluid flow in the presence of vertically placed porous plate and framed dual solutions in the neighborhood of stagnation-point. Viscous BLF is analyzed and reported near stagnation region in two-dimension in studies [23-28].

Published online: January 10 2021

Engineering field has rich and frequent utilization scope of the heat and mass transfer for corporeal mechanisms within physical systems that include diffusive and convective transport. Schmidt [29] and Nusselt [30] identified this analogy for some special conditions and proposed the idea of problem transformation from one domain to the other. It is one of the foremost pillars in the context of mass, momentum and heat transport phenomena. It is prevalent in nature and plays a vital role in engineering design applications, osmosis, transport and absorption of oxygen into the blood, the blood refinement in the liver and kidneys, and in separation processes like membrane filtration, distillation, adsorption, evaporation, precipitation, etc. [31-33]. It is caused by two important mechanisms of diffusion and convection and contributes significantly in multiphase systems. The idea of mass transport enables the researchers for computation of mass flux and distribution over time and space in a system. In order to provide the information on the concentration profile and to describe the process, the mathematical modeling of heat and mass transport processes has been the core of concentration for engineers, numerical analysts and researchers who made a lot of efforts to solve the complexity of flow behaviors and fluid models [34-37].

Electrical appliances such as cooling system or heat exchangers works on the principle of mixed convection flow or free convection which is the focus point of researchers. Stagnation flows along with free convection become more prominent with dominant buoyancy forces and appreciably revamp the thermal fields. Bhargava et al. [38] probed the MHD micro-polar fluid flow with free convection. Anwar et al. [39] conducted a research over MHD natural convection flow near a long vertical plate cuddled in porous medium and observed ramped wall velocity and temperature. Elahi et al. [40] inspected heat transmission over a stretched surface by free convection to conclude numerical solutions. Recent modern world demands high efficiency in modern inventions like cooling and heating systems. Nanofluids with suspending nanoparticles brought an innovation to enhance the thermal convective and conductive heat transfer rates. Sheikholeslami et al. [41] achieve enhanced performance in cooling rates and available energy of solar collectors and scrutinized entropy generation and thermal characteristics by using nanomaterial inside the four-lobed pipe. Sheikholeslami et al. [42] installed helical tape within solar system to analyze nanoparticle turbulent transportation and observe a thinner boundary layer and growth of secondary flow. This phenomenon helps in better mixing of fluid and augments the cooling rate. In comparison with enforced pure convection, significant enhancement or diminish could possible in the regular heat transfer rate and shear stress [43-45]. In the past span of few years, numerous authors impressed with the huge application of convective heat transmission over shrinking surfaces in engineering, heat exchanger, warm air insulation, solar collector and atmospheric flows over boundary layer. The state-of-the-art has been very well summarized in the studies [46-50].

Motivated by the stated facts, the efforts are devoted to scrutinize the heat-mass transmission of non-Newtonian fluid leading to a stretchable layer and neighboring to the stagnation-point flow. To the best of our knowledge this problem has not been studied before and the results reported here are new. Mathematically designed problem is solved by means of Non-linear shooting method (NLSM) and Keller-Box methods, for supporting and contrasting flow. Graphical sketches, analysis and discussions are conducted to accomplish results for temperature, concentration, skin-friction coefficient and velocity. Next to literature review the propound study is furnished as: transport equations and flow analysis is stated in Section 2; solution methodologies are presented in Section 3. The justification of numerical and graphical outcomes is elaborated in Section 4. Finally, essential remarks are communicated in the endmost Section. The outcomes of the study are in ornamental strength with the known findings, which further validate the authenticity of our work. The outcomes of the current study can be utilized to explicate the characteristics of fluids such as exotic lubricants, polymeric fluids, liquid crystals, and animal blood etc.

2. Basic equations and flow analysis

Considering a second-grade fluid in two-dimension near stagnation-point flow with velocity $U_\infty(x)$ towards a vertically continuing stretched sheet set out in the plane $y = 0$. Let the sheet is along horizontal plane and the vertical axis is perpendicular to it as displayed in Fig.1. We presume a linear variation in the velocity $U_w(x)$, surface temperature $T_w(x)$ and concentration $C_w(x)$ with the distance x along the sheet from the stagnation-point, where $T_w(x) > T_\infty$ and $C_w(x) > C_\infty$ with T_∞ used for uniform temperature and C_∞ stands for concentration of the ambient fluid. As the sheet is stretched and origin is kept fixed, two unlike impulsively forces are implemented along the horizontal axis.

In view of assumptions stated above, the transport equations for nonappearance of heat generation and viscous dissipation can be interpreted as follows:

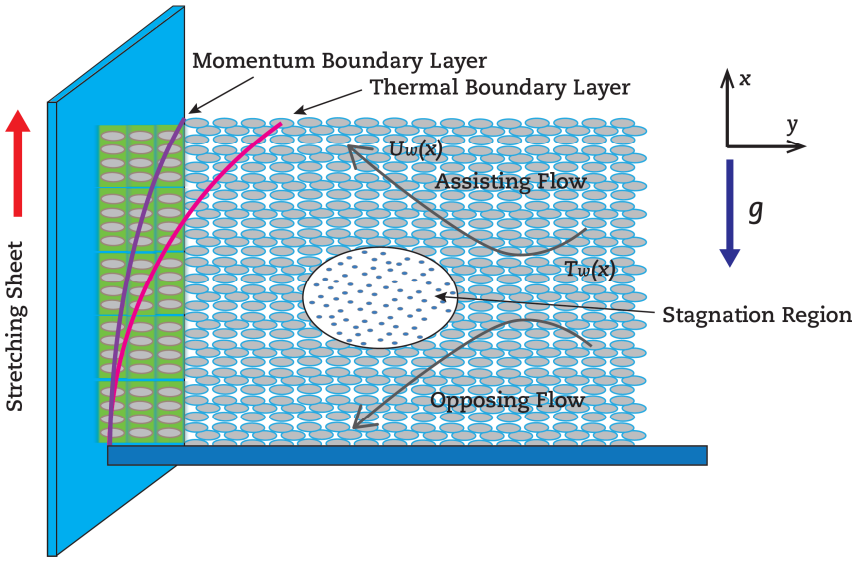

Fig. 1. The orientation of flow and coordinate system

$$\frac{\partial u}{\partial x}+\frac{\partial v}{\partial y}=0, \tag{1}$$

$$u\frac{\partial u}{\partial x}+v\frac{\partial u}{\partial y}=U_\infty\frac{dU_\infty}{dx}+\nu\frac{\partial^2 u}{\partial y^2}+k_0\left[\frac{\partial}{\partial x}\left(u\frac{\partial^2 u}{\partial y^2}\right)+\frac{\partial u}{\partial y}\frac{\partial^2 v}{\partial y^2}+v\frac{\partial^3 u}{\partial y^3}\right]\pm g\beta(T-T_\infty)+g\beta^*(C-C_\infty), \tag{2}$$

$$u\frac{\partial T}{\partial x}+v\frac{\partial T}{\partial y}=\alpha\frac{\partial^2 T}{\partial y^2}, \tag{3}$$

$$u\frac{\partial C}{\partial x}+v\frac{\partial C}{\partial y}=D\frac{\partial^2 C}{\partial y^2}. \tag{4}$$

Subject to the boundary conditions

$$\begin{aligned} &u=U_w(x),\ \ v=0,\ \ T=T_w(x)=T_\infty+\Delta T(x),\\ &C=C_w(x)=C_\infty+\Delta C(x) \qquad\qquad \text{at } y=0,\\ &u\to U_\infty(x),\ \ \frac{\partial u}{\partial y}\to 0,\ T\to T_\infty,\ C\to C_\infty \text{ as } \ y\to\infty. \end{aligned} \tag{5}$$

where horizontal velocity is u, v denotes the velocity in the vertical axis, kinematic viscosity is represented by ν, k_0 stands for viscoelastic parameter, g is acceleration due to gravity, coefficient of thermal diffusivity is denoted by α and D denotes coefficient of mass diffusivity.

In Eq. (2) ' + ' refers assisting and ' – ' shows opposing flow. The flow is due to the inertial and the buoyancy forces. The continuing stretched sheet and free stream velocity are the main cause of inertial forces while varying surface temperature is the major cause for inertial forces.

Stretching surface velocity $U_w(x)$, the surface temperature $\Delta T(x)$, concentration $\Delta C(x)$ and the free stream velocity $U_\infty(x)$ are considered here:

$$U_w(x)=ax,\qquad U_\infty(x)=cx,\qquad \Delta T(x)=bx,\qquad \Delta C(x)=dx. \tag{6}$$

Equations (1)-(4) confess a solution of the form

$$\psi=x\sqrt{a\nu}f(\eta),\quad \eta=\sqrt{\frac{a}{\nu}}y,\quad \theta=\frac{T-T_\infty}{T_w-T_\infty},\quad \phi=\frac{C-C_\infty}{C_w-C_\infty}. \tag{7}$$

Upon making use of Eq. (7) into Eqns. (2)-(4), we get

$$f'''+ff''-f'^2+\lambda\left(2ff'f'''-f''^2-ff^{iv}\right)+\frac{c^2}{a^2}\pm\xi\theta+\xi^*\phi=0, \tag{8}$$

$$\frac{1}{\mathrm{Pr}}\theta''+f\theta'-f'\theta=0, \tag{9}$$

$$\frac{1}{\mathrm{Sc}}\phi''+f\phi'-f'\phi=0. \tag{10}$$

Transforming the boundary conditions into:

$$\begin{aligned} &f(0)=0,\qquad f'(0)=1,\quad \theta(0)=1,\quad \phi(0)=1\\ &f'(\infty)=\frac{c}{a},\quad f''(\infty)=0,\quad \theta(\infty)=0,\quad \phi(\infty)=0. \end{aligned} \tag{11}$$

where

$$\lambda=\frac{ak_0}{\nu},\ \ \mathrm{Pr}=\frac{\nu}{\alpha},\mathrm{Sc}=\frac{\nu}{D},\ \ \xi=\frac{Gr_x}{\mathrm{Re}_x^2},\ \ \xi^*=\frac{Gc_x}{\mathrm{Re}_x^2}. \tag{12}$$

Here λ represents nondimensional viscoelastic parameter, ξ denotes non-dimensional mixed convection parameter, ξ^* is the nondimensional mass convection with $Gr_x=g\beta\Delta T(x)x^3/\nu^2$ and $Gc_x=g\beta\Delta C(x)x^3/\nu^2$ being the local thermal and solutal Grashof number and $\mathrm{Re}_x=U_\infty(x)x/\nu$ the local Reynolds number.

Flow behavior would be analyzed and concluded by examining the local shear stress (skin-friction) with non-dimensional approach, heat transmission rate (Nu_x) and mass transmission rate (Sh_x) at the wall. These influential flow variables are defined as

$$C_{fx}=\frac{2\tau_w}{\rho U_\infty^2},\qquad \mathrm{Nu}_x=\frac{xq_w}{\alpha(T_w-T_\infty)},\mathrm{Sh}_x=\frac{xq_m}{D(C_w-C_\infty)}. \tag{13}$$

where τ_w, q_w and q_m stands for skin-friction, heat transfer and the mass transmission from the surface, which are

$$\tau_w = \mu \left.\frac{\partial u}{\partial y}\right|_{y=0} + k_0 \left[u\frac{\partial^2 u}{\partial x \partial y} + v\frac{\partial^2 u}{\partial y^2} - 2\frac{\partial u}{\partial y}\frac{\partial v}{\partial y}\right]_{y=0},$$
$$q_w = -k\left.\frac{\partial T}{\partial y}\right|_{y=0}, q_m = -m\left.\frac{\partial C}{\partial y}\right|_{y=0}, \tag{14}$$

in which μ, k_0, k and m taken for dynamic viscosity, dimensional viscoelastic parameter, thermal conduction and solutal conductivity respectively. We can obtain by using variables (14),

$$\frac{1}{2}\mathrm{Re}_x^{1/2} C_{fx} = (1+3\lambda) f''(0),\ \mathrm{Re}_x^{-1/2} Nu_x = -\theta'(0),\ \mathrm{Re}_x^{-1/2} Sh_x = -\phi'(0). \tag{15}$$

It is worth portentous here that for $\lambda = 0$ (Newtonian fluids) the system is reduced to the problem presented by Ishak et al [22].

3. Solution methodology

By introducing the new variables U, V, G, P, W, Q, R and S. We can transform the equations (8)-(11) into a set of first order differential equations.

Placing a net on the η defined by

$$\eta_0 = 0,\ \eta_j = \eta_{j-1} + h_j,\ j = 1,2,3,\ldots,J. \tag{16}$$

Now, the quantities (U, V, G , P, W, Q, R, S, f) are approximated at points η_j on the net by (f_j^n , U_j^n , V_j^n , G_j^n , P_j^n , W_j^n , Q_j^n , R_j^n , S_j^n).

For the quantities and points midway the net points, we will use g_j^n

$$\eta_j = \frac{1}{2}\left(\eta_j + \eta_{j-1}\right)$$
$$g_j^{n-1/2} = \frac{1}{2}\left(g_j^n + g_j^{n-1}\right). \tag{17}$$

Now the discretized equations are a system of 9J+9 equations for 9J+9 unknowns f_j^n , U_j^n , V_j^n , G_j^n , P_j^n , W_j^n , Q_j^n , R_j^n , S_j^n , j=0,1,2…J. To linearize these non-linear systems of algebraic equations, Newton's quasi-linearization method is considered as best choice then solution will be approached by using the Keller-box elimination technique.

For the starting of process, the functions f, U, V, G, P, W, Q, R and S are expressed as set of guess profiles, Keller box scheme is is then employed along the boundary layer with second-order accuracy to trek stage by stage. For the difference smaller than 10^{-5} i.e. $|f_i| \le 10^{-5}$ in computing the final velocity, temperature functions and the concentration functions, the iterative procedure is stopped. Where the number of iterations is shown by superscript i. Considering $\eta_j = \sinh(j/a)$, non-uniform grids in the direction direction of η have been incorporated to get quick merging all over the computations, and thus made the computational time and space economic.

Table 1. Numerical values of the skin-friction coefficient for varying Pr when $\xi = 1, c/a = 1, \lambda = 0,\ \xi^* = 0$ and $Sc = 0$.

Pr	Assisting flow			Opposing flow		
	Ishak et al [22]	Hayat et al [43]	Present	Ishak et al [22]	Hayat et al [43]	Present
7.03	0.3645	0.3645	0.3645	-0.3852	-0.3852	-0.3852
10	0.1804	0.1804	0.1804	-0.1832	-0.1833	-0.1832
20	0.1175	0.1175	0.1175	-0.1183	-0.1183	-0.1183
40	0.0873	0.0873	0.0873	-0.0876	-0.0876	-0.0876
60	0.0729	0.0729	0.0729	-0.0731	-0.0731	-0.0731
80	0.0640	0.0641	0.0640	-0.0642	-0.0643	-0.0642
100	0.0578	0.0577	0.0578	-0.0579	-0.0578	-0.0579

Table 2. Numerical values of the Nusselt number for varying Pr when $\xi = 1,\ c/a = 1,\ \lambda = 0,\ \xi^* = 0$ and $Sc = 0$.

Pr	Assisting flow			Opposing flow		
	Ishak et al [22]	Hayat et al [43]	Present	Ishak et al [22]	Hayat et al [43]	Present
7.03	1.0931	1.0931	1.0931	1.0293	1.0293	1.0293
10	3.2902	3.2902	3.2902	3.2466	3.2466	3.2466
20	5.6230	5.6230	5.6230	5.5923	5.5924	5.5923
40	7.9463	7.9464	7.9463	7.9227	7.9227	7.9227
60	9.7327	9.7327	9.7327	9.7126	9.7126	9.7126
80	11.2413	11.2414	11.2413	11.2235	11.2235	11.2235
100	12.5726	12.5725	12.5726	12.5564	12.5565	12.5564

Table 3. Numerical values of the skin-friction coefficient for varying c/a when $\xi = 0,\ \xi^* = 0,\ \lambda = 0, Pr = 1.0$, and $Sc = 0$.

c/a	SKIN FRICTION COEFFICIENT		
	Mahapatar et al [49]	Ishak et al [22]	Present
0.01	-	-0.9980	-0.9980
0.10	-0.9694	-0.9694	-0.9694
0.20	-0.9181	-0.9181	-0.9181
0.50	-06673	-06673	-06673
2.00	2.0175	2.0175	2.0175
3.00	4.7294	4.7294	4.7292
10.00	-	36.2687	36.2687

Table 4. Values of skin friction coefficient and Nusselt number for varying of c/a and ξ when $Pr = 1.0, \lambda = 0.0$ and $\xi^* = 0.0$ and $Sc = 0.0$. (The values in the brackets are from Ishak et al. [23])

c/a	Skin friction coefficient			Nusselt number		
	$\xi = -0.1$	$\xi = 1.0$	$\xi = 10.0$	$\xi = -0.1$	$\xi = 1.0$	$\xi = 10.0$
0.0	-1.0514	-1.5608	2.3041	0.9856	1.0873	1.3715
	(-1.0513)	(-1.5608)	(2.3042)	(0.9856)	(1.0873)	(1.3716)
0.01	-1.0490	-1.5596	2.3049	0.9879	1.0881	1.3719
	(-1.0490)	(-1.5596)	(2.3050)	(0.9880)	(1.0881)	(1.3719)
0.05	-1.0372	-1.5528	2.3094	0.9977	1.0921	1.3734
	(-1.0372)	(-1.5528)	(2.3095)	(0.9977)	(1.0921)	(1.3734)
0.10	-1.0176	-1.5398	2.3177	1.0104	1.0982	1.3756
	(-1.0176)	(-1.5398)	(2.3178)	(1.00079)	(1.0982)	(1.3757)
0.20	-0.9638	-0.5002	2.3432	1.0369	1.1133	1.3813
	(-0.9638)	(-0.5002)	(2.3432)	(1.0362)	(1.1133)	(1.3813)
0.50	-0.7075	-0.2846	2.4887	1.1186	1.1714	1.4057
	(-0.7075)	(-0.2846)	(2.4887)	(1.1186)	(1.1714)	(1.4058)
1.00	-0.0343	0.3350	2.9494	1.2502	1.2827	1.4646
	(-0.0343)	(0.3350)	(2.9495)	(1.2502)	(1.2827)	(1.4646)
2.00	1.9898	2.2913	4.5883	1.4854	1.5020	1.6153
	(1.9899)	(2.2913)	(4.5884)	(1.4855)	(1.5020)	(1.6154)
5.00	11.7323	11.9440	13.6452	2.0416	2.0470	2.0896
	(11.7331)	(11.9449)	(13.6462)	(2.0418)	(2.0473)	(2.0899)

Table 5. Variations in $f''(0), -\theta'(0)$ and $-\varphi'(0)$, for various values of the flow parameters

Pr	λ	c/a	ξ	ξ^*	Sc	$f''(0)$	$-\theta'(0)$	$-\phi'(0)$	$f''(0)$	$-\theta'(0)$	$-\phi'(0)$
						(Assisting flow)			(Opposing flow)		
7.03	1	1	1	1	10	1.2985	3.3601	4.0043	-0.0924	3.3187	3.9586
	2					2.2248	3.3596	4.0038	-0.1623	3.3187	3.9586
	3					3.1138	3.3592	4.0033	-0.2328	3.3187	3.9586
	1	2				6.7447	3.6152	4.2673	5.7564	3.5902	4.2394
		3				11.4035	3.8022	4.4624	10.63	3.7847	4.4427
		1	2			1.956	3.3793	4.0256	-0.8315	3.2963	3.9339
			3			2.5912	3.3977	4.0459	-1.6044	3.2726	3.9077
			1	2		1.8765	3.3757	4.0217	0.5283	3.3359	3.9777
				3		2.4391	3.3908	4.0385	1.1303	3.3524	3.9961
				1	20	1.1569	3.3542	5.6459	-0.25	3.3121	5.5914
					30	1.087	3.3516	6.9051	-0.3272	3.3093	6.8461
10					10	1.2148	4.0002	4.0002	0	3.9631	3.9631
15						1.1277	4.8907	3.9962	0.094	4.8582	3.9674

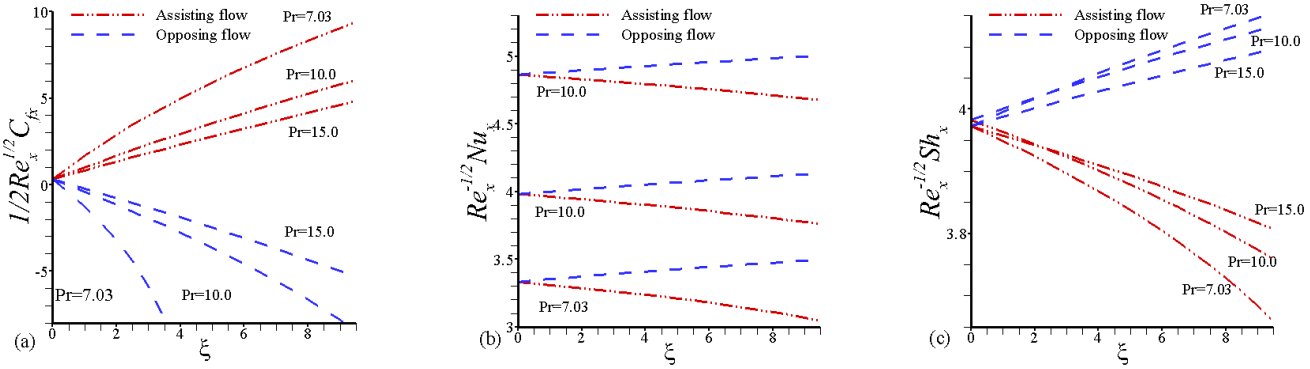

Fig. 2. Influence of Pr on (a) $\frac{1}{2}Re_x^{1/2}C_{fx}$ (b) $Re_x^{-1/2}Nu_x$ (c) $Re_x^{-\frac{1}{2}}Sh_x$ with variation in ξ

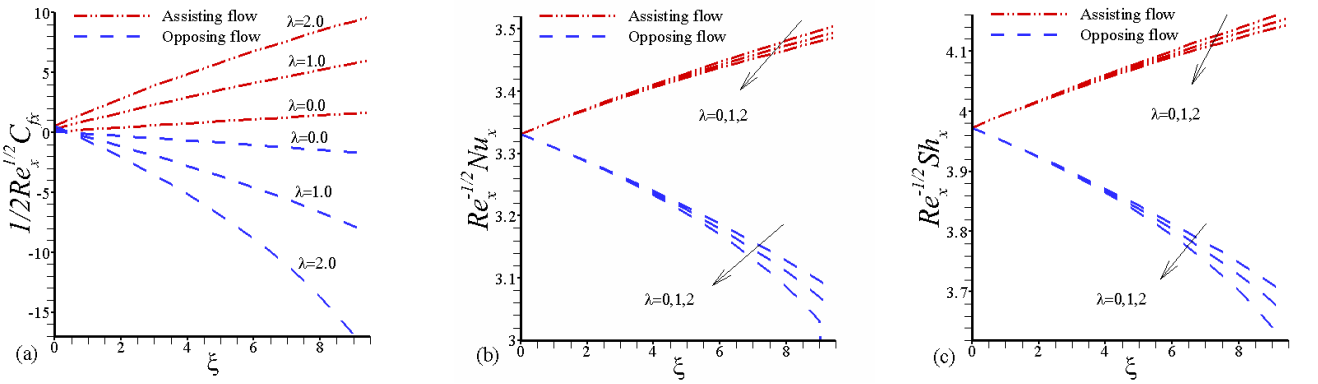

Fig. 3. Influence of λ on (a) $\frac{1}{2}Re_x^{1/2}C_{fx}$ (b) $Re_x^{-1/2}Nu_x$ (c) $Re_x^{-\frac{1}{2}}Sh_x$ with variation in ξ

4. Results and discussion

Non-linear shooting as well as Keller-box methods were employed to numerically solve the transformed system of all 17-20 equations. Tables 1 and 2 enclose a comparative analysis between the coefficients of skin-friction and heat transmission obtained for diverse Pr values, where viscoelastic parameter $\lambda = 0$, solutal buoyancy parameter $\xi^* = 0$, mixed convection parameter $\xi = 1$ and $c/a = 1$. Table 3 compares the values of aforementioned coefficients obtained in the current study with the study of Mahapatra and Gupta [49], and Nazar et al. [22] studies, without any presence of thermal buoyancy $\xi\theta$ and concentration buoyancy forces $\xi^*\varphi$.

Table 4 compares skin friction coefficients and Nusselt numbers obtained for different c/a and ξ values ($Pr = 1.0, \lambda = 0.0, \xi^* = 0$) with those obtained by Ishak et al [23]. High concordance between the outcomes of current and previous investigations encourages to analyze the effects of additional constraints on the characteristics like mass transfer and flow, and heat along heated/continuing stretchable sheet near a stagnation point. Table 5 elaborates the differences of $f''(0), -\varphi'(0)$, and $-\theta'(0)$ for numerous values of dominant flow parameters.

The coefficient of local skin-friction $\mathrm{Re}_x^{1/2} C_{fx}/2$, heat transfer $\mathrm{Re}_x^{-1/2} Nu_x$, mass transfer coefficient $\mathrm{Re}_x^{-1/2} Sh_x$, temperature, concentration and velocity profiles for different physical parameter standards are shown in Figures. 2-11.

4.1 *Effect of physical parameters on above-stated skin-friction coefficient, Nusselt and Sherwood numbers*

Fig. 2 (a-c) elaborates the fluctuations values of the local skin-friction and delineates the Nusselt and Sherwood numbers for varied Pr standards. An increase in ξ stimulates increase in the values of Nusselt numbers, Sherwood numbers and local skin-friction while in the assisting flow case, increase was more prominent/pronounced in comparison of Nusselt number with Sherwood number and skin-friction. Positive correlation of buoyancy force and fluid velocity is the main cause of this increase and elevation in the wall shear stress leads an upsurge in the skin-friction coefficient. These observations were quite opposite for the opposing flow. For a unique ξ value with rising Pr, both the coefficient of skin-friction as well as the Sherwood number of assisting flow decrease, while Nusselt number increases, whereas in opposing flow case, value of all three parameters is raised.

Local Nusselt, skin-friction coefficient and Sherwood numbers are demonstrated in Fig. 3 (a-c) with changing values of λ. In assisting flow case it is observed that the Nusselt values, the skin-friction and Sherwood numbers increase with rising ξ value, while opposing flow showed an opposite trend. With a selected ξ value and increasing λ values for a supporting flow, and increase can be noticed in the skin friction while a decrement in Nusselt and Sherwood numbers. Observing opposing flow under similar conditions of ξ and rising λ values, a decrease can be seen in Nusselt number, Sherwood numbers and skin-friction.

The effect of ξ on the local skin-friction, and the Nusselt and Sherwood numbers is outlined in Fig. 4 (a) to (c). It can be noticed that the Sherwood numbers, skin-friction, and Nusselt number increase by rising c/a values for the assisting flow, while opposing flow displayed an opposite trend. Similarly, at a definite ξ value, a direct correlation can be seen between the c/a value and aforementioned parameters for the supporting flow whereas in contrasting flow this trend is reversed.

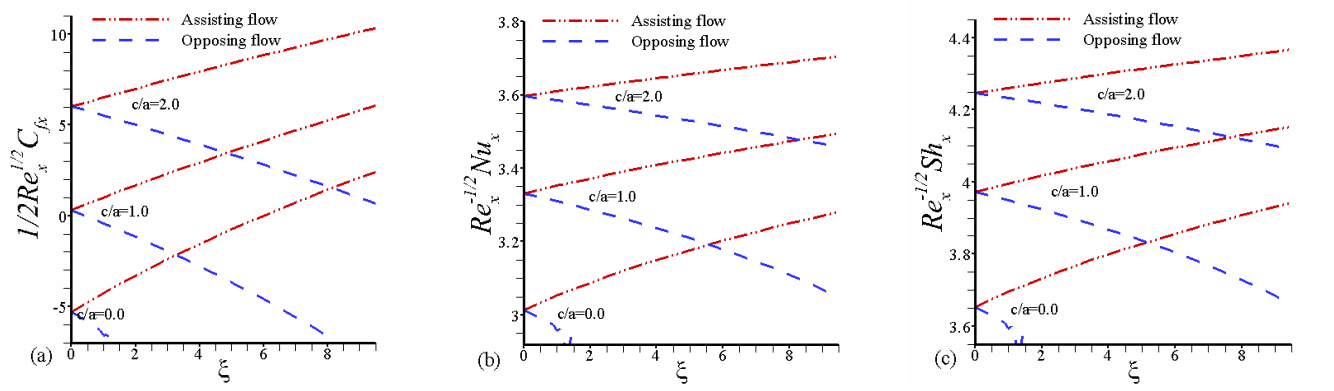

Fig. 4. Influence of c/a on (a) $\frac{1}{2}Re_x^{1/2}C_{fx}$ (b) $Re_x^{-1/2}Nu_x$ (c) $Re_x^{-\frac{1}{2}}Sh_x$ with variation in ξ

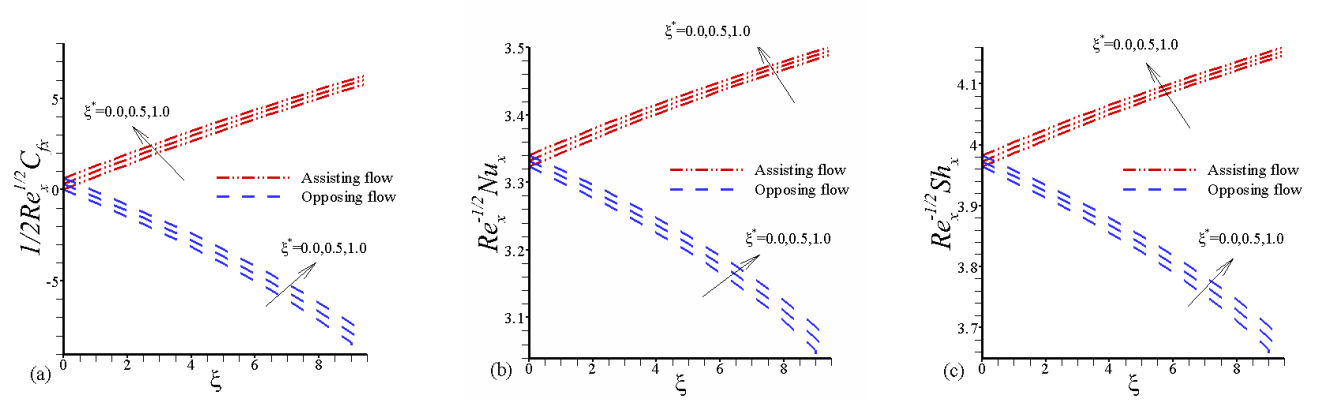

Fig. 5. Influence of ξ^* on (a) $\frac{1}{2}Re_x^{1/2}C_{fx}$ (b) $Re_x^{-1/2}Nu_x$ (c) $Re_x^{-\frac{1}{2}}Sh_x$ with variation in ξ

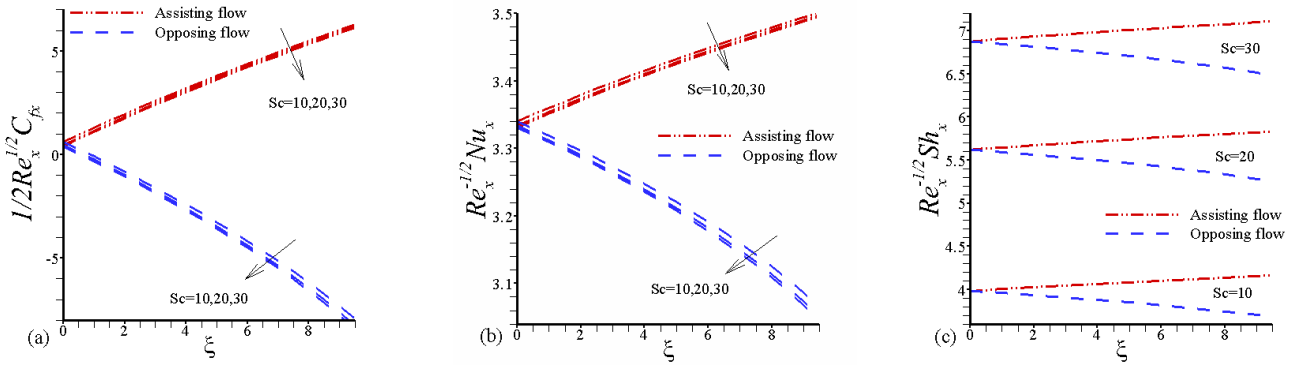

Fig. 6. Influence of Sc on (a) $\frac{1}{2}Re_x^{1/2}C_{fx}$ (b) $Re_x^{-1/2}Nu_x$ (c) $Re_x^{-\frac{1}{2}}Sh_x$ with variation in ξ

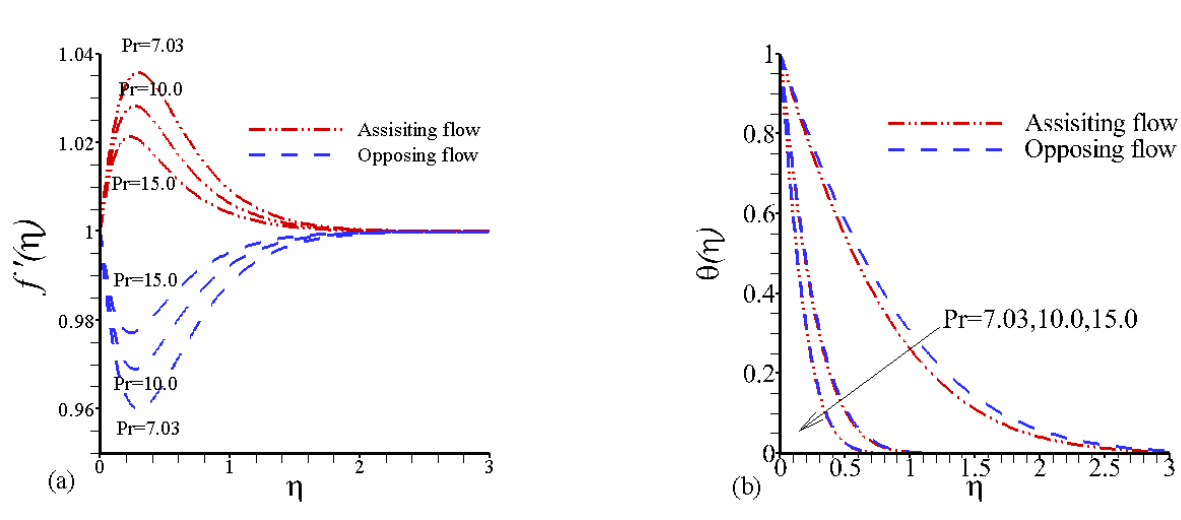

Fig. 7. Influence of Pr on (a) velocity profiles and (b) temperature profiles against η

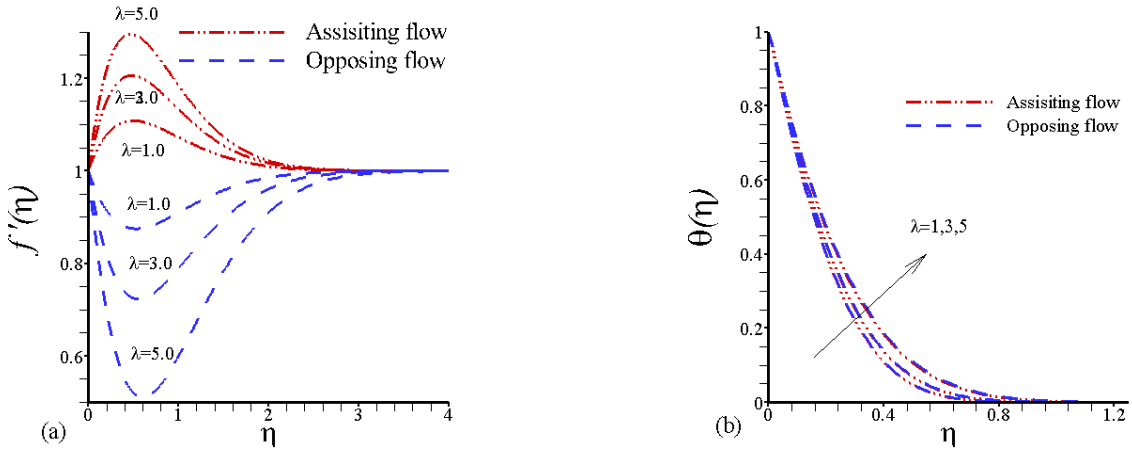

Fig. 8. Influence of λ on (a) velocity profiles and (b) temperature profiles against η

Fig. 5 (a) to (c) is the depiction of variations in the parameters including the Nusselt number, Sherwood numbers and local coefficient of skin friction. Increase in ξ positively affect the parameters in assisting flow whereas reversal in this correlation was observed for opposing flow. Increase in ξ^* with constant value of ξ, increases the parameters for assisting flow however opposite impact is witnessed in the contrasting flow. For various Schmidt number(Sc) values, the effect of ξ on the parameters is shown in Fig. 6 (a) to (c). For the assisting flow, the said parameters are directly related with ξ, while an inverse relation is spotted for the opposing flow. Furthermore, rise in the Sc value for assisting flow at constant ξ develop reduction in the two parameters (skin-friction and Nusselt number) though the Sherwood number is increases. However, the opposing flow showed a reverse trend under similar conditions. Hence, it can be concluded that larger Sc values, for any buoyancy scenario can result in enhanced mass transfer. transfer.

4.2 Influence of corporeal parameters on velocity, temperature and concentration profiles

Figure 7 is the exhibition of the vicissitudes in temperature and velocity of the flow observed against η for various Pr values.

The temperature reducing impact of Pr is clearly visible all over the boundary sheet which culminate in thickness contraction of the thermal boundary layer. From Fig. 7(a), we can easily depict a rise in the assisting flow velocity close to the surface while it declines aside. However, in case of contradictory flow, this behavior is totally opposite. Moreover, decrease in both the velocity as well as span of the momentum, boundary folio of assisting flow is witnessed with rising Pr values. But for opposing flow case, the increase in Pr *causes* velocity to increase while momentum boundary-layer thickness is decreased. In both flows, increase in Pr leads to decline in the thickness of the thermal boundary layer and temperature.

Velocity upsurge in the assisting flow near the surface can also be noticed from Fig. 8(a). However, an opposite behavior is shown by the opposing flow. Additionally, rise in λ elevates the velocity and thickness of the momentum boundary-layer for assisting flow, but a reversal in this behavior is recorded in the opposing flow. Furthermore, Fig. 8(b) clarifies that the rise in λ has no significant effect over thickness and temperature of the thermal layer of boundary.

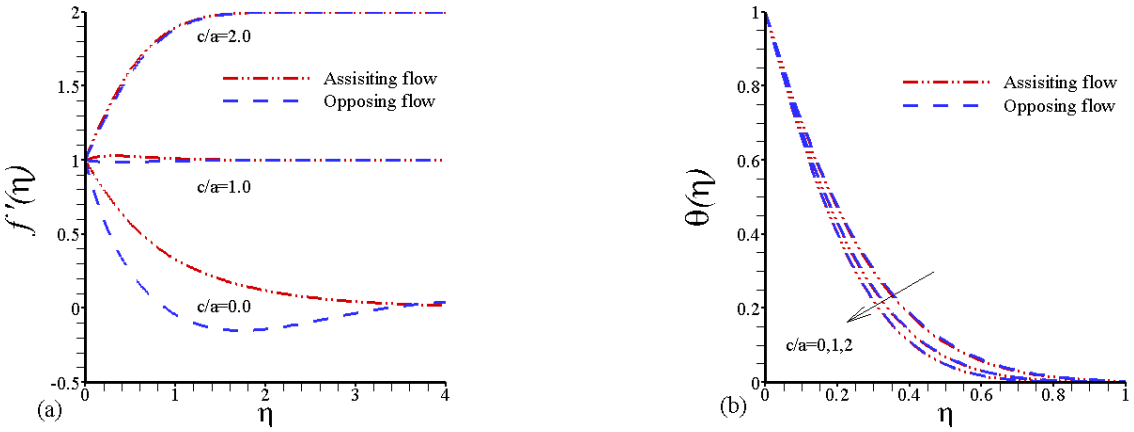

Fig. 9. Influence of c/a on (a) velocity profiles and (b) temperature profiles against η

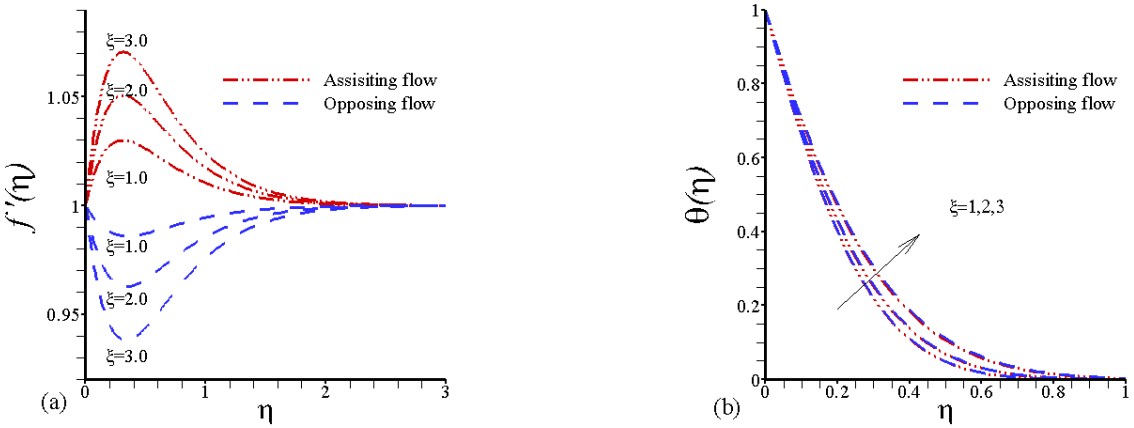

Fig. 10. Influence of ξ on (a) velocity profiles and (b) temperature profiles against η

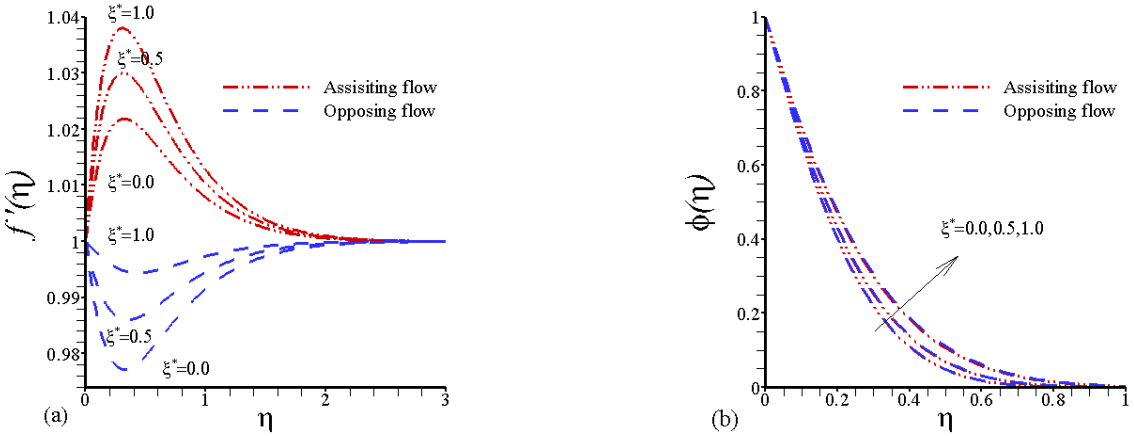

Fig. 11. Influence of ξ^* on (a) velocity profiles and (b) temperature profiles against η

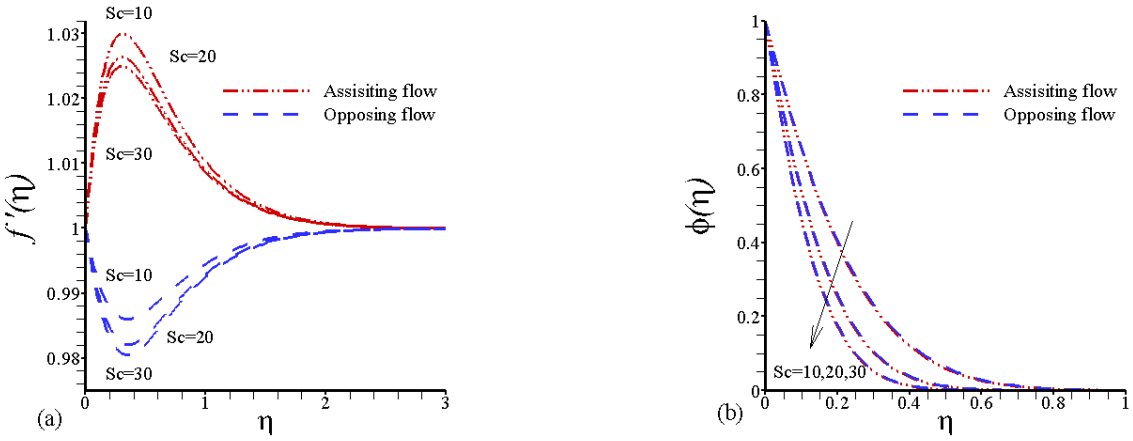

Fig. 12. Influence of Sc on (a) velocity profiles and (b) temperature profiles against η

Figure 9(a) exhibits a decline in thickness of momentum boundary and velocity for both flows when $c/a < 1$ and an incline for $c/a > 1$. The fact is that for a constant value of 'a', a rise in 'c' in relation to 'a' shoots up the straining movement in the neighborhood of stagnation region which results a rise in acceleration of the external stream. As a consequence, boundary layer gets thinner with a rise second-grade c/a. In contrast, the flow reveals overturned boundary layer structure when $c/a < 1$ .It is due to the circumstance that surface velocity ax exceeds the external stream velocity cx. Figure 9(b) indicates a decline in temperature and thickness of thermal boundary-layer for both flows with higher values of c/a.

Figure 10(a) demonstrates that the increase in ξ, increases velocity of assisting flow near the surface which declines at distance. Similarly, along with velocity, girth of the momentum boundary-layer of assisting flow is also increased when ξ increases. Increase in ξ negatively affect both parameters for opposing flow. It is obvious that for $\xi = 0$, the velocity profile will be like pure enforced convection flow. However, for $\xi \geq 1$, the resulting buoyancy force is stable enough to develop a precise and maximum velocity greater enough than that of the free stream; as, forced convection effects are negligible at higher ξ values. Further, Fig. 10(b) indicates that rise in ξ causes decline in the assisting flow temperature and thickness of the thermal boundary-layer, while reverse is true for the opposing flow case. The effect of ξ on temperature was not that pronounced as on velocity.

Figure 11(a) exhibits that velocity of the assisting flow near the surface increases with increasing ξ^* values but it declines with increasing distance from the surface. Similarly, assisting flow velocity and girth of the momentum boundary-layer are directly related with the fluctuations in ξ^*, but an inverse relation is found in opposing flow. Compared to velocity, ξ^* has no significant effect on concentration.

The fluctuations in velocity and concentration profiles against η are demonstrated in Fig. 12 for different Sc values. It can be clearly observed in Fig. 12(b) that the Sc values put negative over the concentration along the boundary layer which consequences in the reduction of thickness of the concentration boundary layer. Furthermore, rise in Sc causes a decrease in the momentum boundary-layer thickness and velocity of assisting flow but for opposing flow, an increase in Sc only increases the velocity whereas thickness of the momentum boundary-layer is decreased. Mass transmission rate was also found in direct relation with Sc. Therefore, concentration decreases with rising Sc values (Fig. 4).

5. Conclusions

The prime objective of current article was to assess the heat and mass transfer of non-Newtonian fluid towards a stretchable surface in the neighborhood of stagnation-point flow. Keller Box scheme was employed in order to solve the considered problem which is one of the most efficient method to tackle the second grade fluids. It can be used to other nonlinear problems in the similar way. The influence of the different flow parameters on the flow filed and temperature was highlighted. We concluded that with rising statistics of ξ, the Sherwood and Nusselt numbers and local skin-friction coefficient raises but compared to Nusselt number, the other two parameters increase faster for the case of assisting flow. The observations were quite opposite in opposing flow case. Moreover, local skin-friction coefficient, the Nusselt and Sherwood numbers showed diverse behavior with the change in values of viscoelastic parameter. In the case of assisting flow, a direct correlation was evident between mixed convection parameter ξ and aforementioned parameters and but for opposing flow, reverse relation was observed. We observed that stagnation flows is important as it modify the flow and thermal fields significantly. It should, however, be mentioned that in such flows, the flow and thermal fields are no longer symmetric with respect to the stagnation line. The outcomes of the current study can be utilized to explicate the characteristics of fluids such as exotic lubricants, polymeric fluids, liquid crystals, and animal blood etc.

Author Contributions

SK and SMI both contributed equally. SK wrote the main manuscript text and performed mathematical modeling. SMI figured out the tables and extract the solution methodology. Both authors contributed in the writing portion of results and discussion and conclusion. They contributed equally in the final version of compilation.

Acknowledgments

We would like to thank Professor Shu Wang for his special assistance, kind support in write up and in the revision of the manuscript. We are grateful to Dr. Rabeah Saeed Kiani for grammar and punctuation check.

Conflict of Interest

The authors declared no potential conflicts of interest with respect to the research, authorship, and publication of this article.

Data availability Statement

All the relevant data is available and can be provided on demand.

Funding

This effort received funding from the National Natural Science Foundation of China, Grant/ Award Number: 11271037.

Nomenclature

Pr	Prandtl number	$U_\infty(x)$	Free stream velocity
λ	Viscoelastic Parameter	t	Time
C_{f_x}	Skin friction coefficient	Gr_x	Local Grashof number
Nu_x	Local Nusselt number	D	Mass diffusitivity coefficient
Re_x	Local Reynolds number	Re	Reynold number
ξ	Mixed convection parameter	$\Delta C(x)$	Concentration
ξ^*	Mass convection parameter	ν	Kinematic Viscosity
$U_w(x)$	Stretching surface velocity	$\Delta T(x)$	Surface Temperature

Greek Symbols

μ	Dynamic viscosity	m	Solutal conductivity
ρ	Fluid density	α	Thermal Diffusitivity
k	Thermal conduction parameter	g	Gravitational acceleration
k_0	Dimensional viscoelastic parameter	λ	Mixed Convection Parameter

References

[1] Sakiadis, B. C. Boundary-layer behavior on continuous solid surfaces: I. Boundary-layer equations for two-dimensional and axisymmetric flow. *AIChE Journal*, *7*(1), 1961, 26-28.
[2] Crane, L. J., Flow past a stretching plate. *Zeitschrift für Angewandte Mathematik und Physik ZAMP*, *21*(4), 1970, 645-647.
[3] Erickson, L. E., Fan, L. T., & Fox, V. G., Heat and mass transfer on moving continuous flat plate with suction or injection. *Industrial & Engineering Chemistry Fundamentals*, 5(1), 1966, 19-25.
[4] Gupta, P. S., & Gupta, A. S., Heat and mass transfer on a stretching sheet with suction or blowing. *The Canadian Journal of Chemical Engineering*, 55(6), 1977, 744-746.
[5] Grubka, L. J., & Bobba, K. M., Heat transfer characteristics of a continuous stretching surface with variable temperature. *ASME J. Heat Transfer*, *107*(1), 1985, 248-250.
[6] Char, M. I., Heat transfer of a continuous, stretching surface with suction or blowing. *Journal of Mathematical Analysis and Applications*, *135*(2), 1988, 568-580.
[7] M.E. Ali. Heat transfer characteristics of a continuous stretching surface. *Heat Mass Transfer*, 29, 1994, 227-234.
[8] Chen, C. H., Laminar mixed convection adjacent to vertical, continuously stretching sheets. *Heat and Mass Transfer*, *33*(56), 1998, 471-476.
[9] Wang, C. Y., Analysis of viscous flow due to a stretching sheet with surface slip and suction. *Nonlinear Analysis: Real World Applications*, *10*(1), 375-380.
[10] Cortell, R., MHD flow and mass transfer of an electrically conducting fluid of second grade in a porous medium over a stretching sheet with chemically reactive species. *Chemical Engineering and Processing: Process Intensification*, *46*(8), 2009, 721-728.
[11] Cortell, R., Toward an understanding of the motion and mass transfer with chemically reactive species for two classes of viscoelastic fluid over a porous stretching sheet. *Chemical Engineering and Processing-Process Intensification*, *46*(10), 2007, 982-989.
[12] Mansour, M. A., El-Anssary, N. F., & Aly, A. M., Effects of chemical reaction and thermal stratification on MHD free convective heat and mass transfer over a vertical stretching surface embedded in a porous media considering Soret and Dufour numbers. *Chemical Engineering Journal*, 145(2), 2008, 340-345.
[13] Hayat, T., Abbas, Z., & Ali, N., MHD flow and mass transfer of a upper-convected Maxwell fluid past a porous shrinking sheet with chemical reaction species. *Physics Letters A*, *372*(26), 2008, 4698-4704.
[14] Bhattacharyya, K., & Layek, G. C., Chemically reactive solute distribution in MHD boundary layer flow over a permeable stretching sheet with suction or blowing. *Chemical Engineering Communications*, *197*(12), 2010, 1527-1540.
[15] Hiemenz, K. , Die Grenzschicht an einem in den gleichformigen Flussigkeitsstrom eingetauchten geraden Kreiszylinder. *Dinglers Polytech. J.*, *326*, 1911, 321-324.
[16] TC, Chiam., Stagnation-point flow towards a stretching plate. *Journal of the Physical Society of Japan*, *63*(6), 1994, 2443-2444.
[17] Nazar, R., Amin, N., Filip, D., & Pop, I., Stagnation point flow of a micropolar fluid towards a stretching sheet. *International Journal of Non-Linear Mechanics*, *39*(7), 2004, 1227-1235.
[18] Layek, G. C., Mukhopadhyay, S., & Samad, S. A., Heat and mass transfer analysis for boundary layer stagnation-point flow towards a heated porous stretching sheet with heat absorption/generation and suction/blowing. *International Communications in Heat and Mass Transfer*, 34(3), 2007, 347-356.
[19] Nadeem, S., Hussain, A., & Khan, M., HAM solutions for boundary layer flow in the region of the stagnation point towards a stretching sheet. *Communications in Nonlinear Science and Numerical Simulation*, 15(3), 2010, 475-481.
[20] Singh, J., Mahabaleshwar, U. S., & Bognár, G., Mass transpiration in nonlinear MHD flow Due to porous Stretching Sheet. *Scientific Reports*, 9(1), 2019, 1-15.
[21] Hayat, T., Abbas, Z., Pop, I., & Asghar, S., Effects of radiation and magnetic field on the mixed convection stagnation-point flow over a vertical stretching sheet in a porous medium. *International Journal of Heat and Mass Transfer*, *53*(1-3), 2010, 466-474.
[22] Ishak, A., Nazar, R., Arifin, N. M., & Pop, I., Dual solutions in mixed convection flow near a stagnation point on a vertical porous plate. *International Journal of Thermal Sciences*, *47*(4), 2008, 417-422.
[23] Ishak, A., Nazar, R., & Pop, I., Mixed convection boundary layers in the stagnation-point flow toward a stretching vertical sheet. *Meccanica*, 41(5), 2006, 509-518.
[24] Ishak, A., Nazar, R., Arifin, N. M., & Pop, I., Mixed convection of the stagnation-point flow towards a stretching vertical permeable sheet. *Malaysian Journal of Mathematical Sciences*, *2*, 2007, 217-226.
[25] Garg, V. K., & Rajagopal, K. R., Stagnation point flow of a non-Newtonian fluid. *Mechanics Research Communications*,17(6), 1990, 415-421.
[26] Wang, C. Y., Stagnation flow towards a shrinking sheet. *International Journal of Non-Linear Mechanics*, 43(5), 2008, 377-382.
[27] M. Awais, T. Hayat, M. Mustafa, K. Bhattacharyya, M. A. Farooq., Analytic and numeric solutions for stagnation-point flow with melting, thermal-diffusion and diffusion-thermo effects. *International Journal of Numerical Methods Heat Fluid Flow*, 24(2), 2014, 438-454.

[28] T. Hayat, Z. Iqbal, M. Mustafa, A. Alsaedi., Stagnation-point flow of Jerey fluid with melting heat transfer and Soret and Dufour effects. *International Journal of Numerical Methods for Heat and Fluid Flow*, 24(2), 2014, 402-418.
[29] Schmidt, E., Verdunstung und wärmeübergang. *International Journal of Heat and Mass Transfer*, 19(1), 1976, 3-8.
[30] Nusselt, W., Wärmeübergang, diffusion und verdunstung. *ZAMM-Journal of Applied Mathematics and Mechanics/Zeitschrift für Angewandte Mathematik und Mechanik*, *10*(2), 1930, 105-121.
[31] Damtie, M. M., Woo, Y. C., Kim, B., Park, K. D., Hailemariam, R. H., Shon, H. K., & Choi, J. S., Analysis of mass transfer behavior in membrane distillation, Mathematical modeling under various conditions. *Chemosphere*, *236*, 2019, 124289.
[32] Yaïci, W., & Entchev, E., Coupled unsteady computational fluid dynamics with heat and mass transfer analysis of a solar/heat powered adsorption cooling system for use in buildings. *International Journal of Heat and Mass Transfer*, *144*, 2019, 118648.
[33] Das, K., Effects of thermophoresis and thermal radiation on MHD mixed convective heat and mass transfer flow. *Afrika Matematika*, *24*(4), 2013, 511-524.
[34] De, P., Mondal, H., & Bera, U. K., Influence of nanofluids on magnetohydrodynamic heat and mass transfer over a non-isothermal wedge with variable viscosity and thermal radiation. *Journal of Nanofluids*, *3*(4), 2014, 391-398.
[35] Pal, D., & Mandal, G., Influence of thermal radiation on mixed convection heat and mass transfer stagnation-point flow in nanofluids over stretching/shrinking sheet in a porous medium with chemical reaction. *Nuclear Engineering and Design*, *273*, 2014, 644-652
[36] Alam, M. S., Rahman, M. M., & Sattar, M. A., MHD free convective heat and mass transfer flow past an inclined surface with heat generation. *Science & Technology Asia*, 2006, 1-8.
[37] Pal, D., & Mondal, H., Soret-Dufour Effects on Hydromagnetic Non-Darcy Convective-Radiative Heat and Mass Transfer over a Stretching Sheet in Porous Medium with Viscous Dissipation and Ohmic Heating. *Journal of Applied Fluid Mechanics*, *7*(3), 2014, 513–523.
[38] Bhargava, R., Kumar, L., & Takhar, H. S., Numerical solution of free convection MHD micropolar fluid flow between two parallel porous vertical plates. *International Journal of Engineering Science*, *41*(2), 2003, 123-136.
[39] Anwar, T., Kumam, P., & Watthayu, W., An exact analysis of unsteady MHD free convection flow of some nanofluids with ramped wall velocity and ramped wall temperature accounting heat radiation and injection/consumption. *Scientific Reports*, *10*(1), 2020, 1-19.
[40] Ellahi, R., Zeeshan, A., Shehzad, N., & Alamri, S. Z., Structural impact of Kerosene-Al2O3 nanoliquid on MHD Poiseuille flow with variable thermal conductivity: application of cooling process. *Journal of Molecular Liquids*, *264*, 2018, 607-615.
[41] Sheikholeslami, M., et al. Performance of solar collector with turbulator involving nanomaterial turbulent regime. *Renewable Energy*, *163*, 2021, 1222-1237.
[42] Sheikholeslami, M., and Seyyed Ali, F., Nanoparticle transportation inside a tube with quad-channel tapes involving solar radiation. *Powder Technology, 378*, 2021, 145-159.
[43] Hayat, T., Abbas, Z., & Pop, I., Mixed convection in the stagnation point flow adjacent to a vertical surface in a viscoelastic fluid. *International Journal of Heat and Mass Transfer*, 51(11-12), 2008, 3200-3206.
[44] N. Ramachandran, T.S. Chen, B.F. Armaly., Mixed convection in stagnation flows adjacent to vertical surfaces. *ASME J. Heat Transfer*, 110, 1988, 373–377.
[45] Lok, Y. Y., Amin, N., Campean, D., & Pop, I., Steady mixed convection flow of a micropolar fluid near the stagnation point on a vertical surface. *International Journal of Numerical Methods for Heat & Fluid Flow,* 15, 2005, 654–670.
[46] Golafshan, B., & Rahimi, A. B., Effects of radiation on mixed convection stagnation-point flow of MHD third-grade nanofluid over a vertical stretching sheet. *Journal of Thermal Analysis and Calorimetry*, 135(1), 2019, 533-549.
[47] Ali, M. E., The effect of variable viscosity on mixed convection heat transfer along a vertical moving surface. *International Journal of Thermal Sciences*, 45(1), 2006, 60-69.
[48] Ali, M., & Al-Yousef, F., Laminar mixed convection from a continuously moving vertical surface with suction or injection. *Heat and Mass Transfer*, 33(4), 1998, 301-306.
[49] Mahapatra, T. R., Gupta, A. S., Heat transfer in stagnation-point flow towards a stretching sheet. *Heat Mass Transfer*, 38, 2002, 517-521.
[50] Kudenatti, R. B., Hydrodynamic flow of non-Newtonian power-law fluid past a moving wedge or a stretching sheet: a unified computational approach. *Scientific Reports*, *10*(1), 2020, 1-16.

ORCID iD

Sudheer Khan https://orcid.org/0000-0002-7502-9081
Syed Muhammad Imran https://orcid.org/0000-0001-5438-4650

How to cite this article: Khan S., Imran S.M., Wang S. Diffusion-thermo Effects in Stagnation Point Flow of Second Grade Fluid past a Stretching Plate, *J. Appl. Comput. Mech.*, 7(2), 2021, 902–912. https://doi.org/10.22055/JACM.2021.35332.2630